


## Polaron-induced upconversion from triplets to singlets: Fluorescence- and phosphorescence-resolved optically detected magnetic resonance of OLEDs

F. Braun<sup>1</sup>, T. Scharff, T. Grünbaum<sup>1</sup>, E. Schmid<sup>1</sup>, S. Bange, V.V. Mkhitarian<sup>1</sup>,\* and J.M. Lupton  
*Institut für Experimentelle und Angewandte Physik, Universität Regensburg, Universitätsstraße 31, 93053  
 Regensburg, Germany*

 (Received 1 November 2022; revised 2 October 2023; accepted 4 October 2023; published 30 October 2023)

The modest spin-orbit coupling arising from the  $n\text{-}\pi^*$  transitions of phenazine complexes offers the unique means to activate the dual emission of singlets and triplets, i.e., fluorescence and phosphorescence, in organic light-emitting diodes (OLEDs) at room temperature. By spectrally resolving OLED electroluminescence, we investigate the optically detected magnetic resonance (ODMR) of such a metal-free dual-emitting host-guest OLED in separate fluorescence and phosphorescence channels. The phosphorescence component of ODMR exhibits two distinctive resonance lineshapes, which differ between the in-phase and quadrature channels. To rationalize these features, we devise a comprehensive quantum stochastic model relating the phase-sensitive components of the lock-in-detected ODMR signal to the forward and reverse transfer of triplets between the host molecules of the OLED, where they are dark, and the guest molecules, from which phosphorescence occurs. Within the model proposed, the observed resonance lines result from the interplay of spin-dependent electron-hole polaron-pair (PP) recombination and triplet-exciton-polaron (TEP) reaction processes. The analytical description of the model is based on the stochastic Liouville equation treatment of the PP and TEP spin dynamics. Quantitative analysis is performed by means of numerical simulations exploiting solutions of the corresponding Liouville equations based on Floquet theory. The resulting accurate match to experiments allows us to draw plausible conclusions with regards to the numerical values of parameters that characterize the system, including the phosphorescence lifetime and the polaron hyperfine interaction strengths. Based on the theoretical framework used to describe the phosphorescence ODMR lineshape, we compute the resonance line recorded in the conjugated detection channel, i.e., in the fluorescence. Surprisingly, this analysis reveals a substantial contribution of the TEP mechanism to the singlet fluorescence channel, implying that fluorescent species are generated from triplets in the course of the TEP reaction. We argue that the TEP process occurring in our device is a spin-allowed polaron-assisted upconversion of triplets to singlets, in which free polarons scatter off trapped triplets, losing their energy to transfer triplets to singlets of higher energy.

DOI: [10.1103/PhysRevApplied.20.044076](https://doi.org/10.1103/PhysRevApplied.20.044076)

### I. INTRODUCTION

Unraveling the mechanisms of the generation of luminescent species controlling the optoelectronic properties of organic light-emitting diodes (OLEDs) aids both fundamental research and technology. An ideal spectroscopic tool for the investigation of these mechanisms and their interrelation with device resistance is offered by optically and electrically detected magnetic resonance (ODMR and EDMR), with a sensitivity exceeding that of traditional electron paramagnetic resonance (EPR) by many orders of magnitude [1]. In combination with rigorous theoretical lineshape analysis, ODMR and EDMR can provide insights into the carrier-interaction mechanisms responsible for the generation of light that are

inaccessible by any other spectroscopic means. Here, we report on a room-temperature ODMR study of a metal-free dual fluorescence- and phosphorescence-emitting OLED, advancing the prior limitations of ODMR by spectroscopically dispersing the luminescence. The ability to separate fluorescence and phosphorescence opens up possibilities for the investigation of interconversion processes of singlet- and triplet-exciton species coexisting in a single device. Separating fluorescence and phosphorescence in a dual singlet-triplet emitter device may provide direct spectroscopic access to the singlet-triplet intersystem crossing, singlet fission, triplet-triplet annihilation, and other fundamental processes governing the optoelectronic properties. Dual emitters offer a window to spin correlations and spin-relaxation channels, which, in turn, can be highly sensitive to magnetic fields [1–4]. For the best use of dual emitters as local probes of spin-dependent processes, it is crucial to achieve fluorescence

\*vmkhitar@gmail.com

and phosphorescence from one and the same molecule at comparable emission intensities and with minimal spectral overlap between the two species. In general, the observation of phosphorescence in organic materials is challenging because the triplet-exciton recombination responsible for such an emission violates spin conservation. The spin-forbidden phosphorescence is possible in the presence of a spin-orbit interaction (SOI), which is generally small in organic materials due to the light constituent elements. In organometallic emitters, a sufficient SOI for the long-lived triplet state is realized by incorporating heavy atoms [5–7]. However, in these systems, intersystem crossing is enhanced to such an extent that the singlet state is depleted, and phosphorescence dominates over fluorescence. Incorporating trace amounts of covalently bound heavy atoms into polymeric materials offers another route to achieving phosphorescence but results in a triplet-diffusion-limited inhomogeneous system that cannot probe fluorescence and phosphorescence yields directly [8]. A compromise in the strength of the SOI and the magnitude of transition dipole moments has been found by invoking all-organic phenazine-based emitters [9,10], where the SOI is weaker than in organometallic complexes due to the low atomic order number of the constituent elements. By embedding the 11,12-dimethyldibenzo[*a,c*]phenazine (DMDB) emitter in a typical OLED host, a balanced dual emission arises from a single chromophore with well-separated fluorescence and phosphorescence spectral components [10].

We fabricated metal-free dual-emitting OLEDs based on an emitting layer consisting of 4,4'-bis(*N*-carbazolyl)-1,1'-biphenyl (CBP) and DMDB, with a ratio of 97:3 by weight, and performed ODMR measurements. In our experiment, the changes in the device fluorescence and phosphorescence induced by magnetic resonance were separated and measured via a lock-in technique. We utilized a radio-frequency (rf) drive with a carrier frequency of 280 MHz, inducing spin-1/2 electron-spin resonance in a static magnetic field of roughly 10 mT. In this domain, electron- and hole-polaron-spin hyperfine couplings with the local hydrogen nuclear spins, which are typically in the order of 1 mT in strength, are not completely screened out by the external field. As a result of an improved device structure compared to our earlier attempts at such a dual-emitter ODMR [3], high-quality ODMR lines are recorded, allowing us to assess the different effects of magnetic resonance on the charge-carrier spins in the fluorescence and phosphorescence channels. Moreover, both the in-phase (i.e., instantaneous) and quadrature (i.e., delayed) components of the phosphorescence ODMR are of high resolution and amenable to theoretical lineshape analysis. The unusual shapes of the phosphorescence ODMR lines recorded are correctly reproduced theoretically, by involving three distinct processes: polaron-pair (PP) [8,11–16] recombination in the host matrix, PP recombination situated around a guest emitter

molecule, and a triplet-exciton-polaron (TEP) reaction [1,2,11,17–20] of phosphorescent (guest) triplet excitations with hole polarons on guest molecules. These three processes are interrelated within a bigger model of the host-guest triplet-exciton transfer, some characteristic parameters of which are found by combining the lineshape analysis with the analytical treatment of the lock-in response. The model allows us to elucidate the following key observations: (i) the in-phase and out-of-phase components of phosphorescence ODMR apparently have different lineshapes; and (ii) despite the reported long phosphorescence lifetime [10] of about 97 ms, the in-phase component of the lock-in-detected phosphorescence signal is dominant over the out-of-phase one, at a reference modulation period of 10.8 ms. This observation is surprising as, in general, one would expect the in-phase signal to contain the components of the response to rf excitation that are faster than the modulation period, whereas slower processes would contribute predominantly to the out-of-phase channel.

Even more intriguing is the result that the fluorescence resonance line cannot be reproduced theoretically by merely combining the guest and host PP processes, which are the prime channels of singlet-exciton generation from electrically injected electron-hole pairs, but instead it is fitted very closely with a combination of the PP and TEP resonance lines of the guest molecules. This result clearly indicates that, besides the guest PP recombination process, fluorescent species are generated in the TEP process. A feasible scenario of TEP-induced singlet generation is triplet upconversion, where free polarons scatter off trapped triplet excitons, losing their energy to triplets and causing the triplets to cross to the singlet manifold [2,17–19,21]. The absence of delayed fluorescence by triplet-triplet annihilation in our OLEDs offers further support for TEP-induced triplet upconversion, which requires a high-energy polaron, and therefore, cannot contribute to delayed fluorescence.

The polaron-assisted triplet-exciton upconversion process is spin selective and occurs from the doublet state of the triplet-polaron complex. A somewhat different spin-selective TEP process is the quenching of triplet excitons by trapped polarons with the subsequent detrapping of the polaron, which has also been discussed extensively in the literature [1,11,20]. The TEP-induced upconversion and quenching processes are illustrated in Fig. 1. Although they involve microscopically different electronic transitions, they both constitute triplet-deactivation processes with equivalent spin dynamics and induce an identical magnetic field dependence in the triplet-exciton population. Therefore, these processes are indistinguishable when merely considering the phosphorescence channel of ODMR. By scrutinizing the fluorescence ODMR spectrum in addition to the phosphorescence, the TEP process found in our devices through the analysis of the

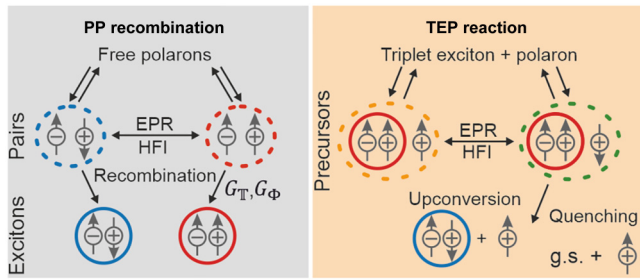


FIG. 1. Illustration of possible spin-dependent pathways of exciton generation in OLEDs. Left, PP mechanism of exciton generation on the host and guest molecules. Spin multiplicity of weakly coupled electron-hole spin-pair states (dashed ovals) is altered between singlet (blue) and triplet (red) either internally, by a hyperfine interaction (HFI) of polaron spins with surrounding nuclear spins, or externally, by EPR. Triplet exciton yields per unit time on the host and guest molecules,  $G_T$  and  $G_\Phi$ , constitute the triplet-generation rates that define the model described by Eq. (3). Right, two different TEP mechanisms of triplet quenching and triplet upconversion share the same scheme of spin dynamics. Total spin of the TEP precursor states (dashed ovals) is mixed between quartet (orange) and doublet (green) by either the HFI or EPR. Apart from this mixing, the quartet state can dissociate back into a separate triplet exciton and polaron, while the doublet can also recombine into a polaron and a singlet. In the case of TEP upconversion, the recombination product is a singlet exciton (blue) and a lower-energy polaron, whereas it is a ground state (g.s.) and a higher-energy polaron in the case of TEP quenching.

phosphorescence ODMR spectra is confirmed to arise due to upconversion.

This observation of the TEP process provides additional insight into the mechanism, besides previous reports on a triplet half-field resonance in the EDMR at X-band frequencies ( $\sim 10$  GHz) and low temperatures [1], and a direct measurement of the spin quantum number of the interacting species by quantification of the Rabi frequency under coherent drive [22]. In fact, time-resolved pulsed EDMR experiments under these conditions allow a direct distinction between the PP mechanism and the TEP process through the Rabi frequency [22]. In conventional OLEDs, the triplet half-field signal, and hence, direct signature of the TEP mechanism, is generally lost at room temperature, where the triplets are quenched. This limitation should not apply to the dual-emitter OLEDs employed here, since they clearly show phosphorescence, but, as discussed in detail here, we do not expect to be able to resolve a half-field resonance at the extremely low resonance frequencies employed in the present study.

## II. METHODS AND EXPERIMENTAL RESULTS

At the heart of the measurement technique utilized in this study is the simultaneous detection of fluorescence

and phosphorescence from an OLED. Details of the structure of the OLED, which is optimized for the best ODMR signal quality, are given in the Supplemental Material [23].

The experiment is illustrated in Fig. 2. Simultaneous optical detection is achieved by feeding the luminescence signal into a dichroic mirror, splitting the spectrum at 552 nm. Additionally, a set of optical filters are used to reduce leakage from fluorescence into the phosphorescence channel and to filter out the residual emission from the OLED matrix material. Although the spectra are quite broad, we have previously demonstrated that they do not overlap sufficiently to obscure quantitative measurements of the changes of singlet and triplet yields—in fact, spin-polarization experiments on OLEDs reveal a perfect 3:1 ratio of triplets to singlets, just by quantifying the spectral amplitudes [24]. EL is recorded under magnetic resonance conditions, where the device is operated in a static magnetic field,  $\mathbf{B}_0$ , created by a set of Helmholtz coils, and under an rf excitation,  $\mathbf{B}_{rf}(t)$ , oriented perpendicular to  $\mathbf{B}_0$ , created by a stripline connected to an rf source. A standard

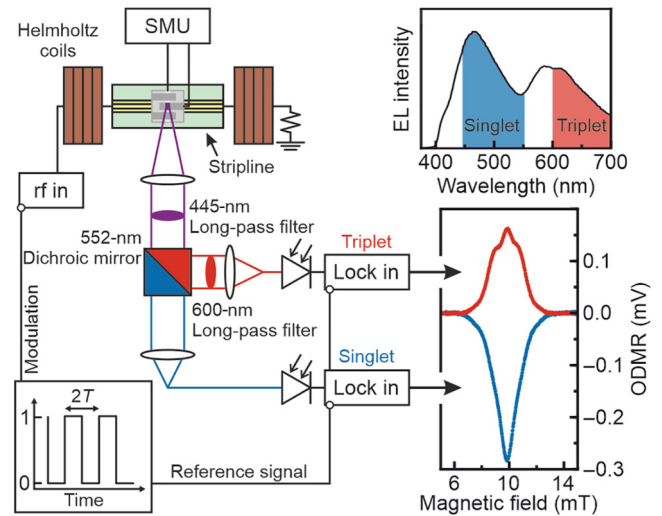


FIG. 2. Schematic of the experiment. OLED is driven at a constant current of  $500 \mu\text{A}$  by a source-measure unit (SMU). Set of Helmholtz coils and a stripline connected to an rf source create the static and oscillating magnetic fields needed for the magnetic resonance measurement. Luminescence from the device is captured and fed through a set of optical filters to achieve the separation of singlet (fluorescence) and triplet (phosphorescence) contributions and is ultimately measured by two separate photodiodes connected to two lock-in amplifiers. Electroluminescence (EL) spectrum with distinct fluorescence (blue) and phosphorescence (red) regions is shown on the upper right (white areas are blocked out by the filters). Recorded fluorescence (blue) and phosphorescence (red) in-phase ODMR signals are presented on the lower right. Rectangular rf amplitude modulation is shown on the lower left. Note the extremely low resonance field of 10 mT and the correspondingly low resonance frequency. Measurement is only sensitive to spin-1/2, i.e., polaron, resonances.

lock-in measurement scheme involving a modulated rf excitation,

$$B_{\text{rf}}(t) = F(t)B_1 \sin(\omega_0 t), \quad (1)$$

is implemented, where  $F(t)$  is the rectangular modulation, which is time periodic with a period  $2T$ ,

$$\begin{aligned} F(t) &= 1, & 0 \leq t < T, \\ F(t) &= 0, & T \leq t < 2T, \end{aligned} \quad (2)$$

extended periodically over time  $t > 2T$ . In this study, the modulation half-period was chosen to be  $T \approx 5.4$  ms. The fluorescence and phosphorescence signals are then demodulated by two separate lock-in amplifiers, yielding the in-phase and out-of-phase components of the rf-induced signals. With an rf carrier frequency of  $\omega_0/2\pi \simeq 280$  MHz, the ODMR lines are detected around static field values of  $B_0 \simeq 10$  mT.

The ODMR spectra recorded are shown in Fig. 3 (see also the lower right of Fig. 2). The in-phase triplet ODMR spectrum has a rather peculiar lineshape. The shoulder-like features around the central peak appear to contradict the conventional observation from previous OLED ODMR studies that the ODMR signals can be modeled by a superposition of two Gaussians with different linewidths [1,25], arising from the two hyperfine distributions experienced by the electron and hole. This peculiar lineshape, as well as the apparent lack of a quantitative anticorrelation between

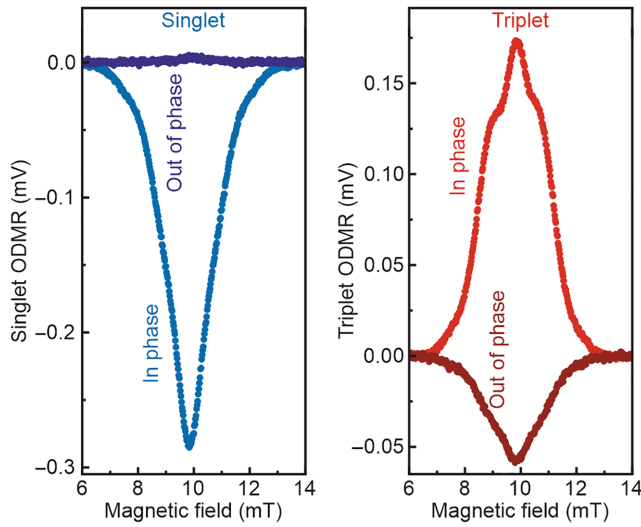


FIG. 3. Experimental ODMR spectra in the fluorescence (left) and phosphorescence (right) channels. Different shapes are observed for the in-phase and out-of-phase phosphorescence lines. Because of the short lifetime of singlet excitons, the out-of-phase fluorescence component has a poor signal-to-noise ratio and is not suitable for theoretical analysis. Under the given experimental conditions, the resonances correspond to spin-1/2 species.

the singlet and triplet channels, which is in contrast to prior observations made for different materials [8], are addressed within the following theoretical treatment.

### III. MODELING OF ODMR

#### A. Global model

The recorded resonance lines are correctly reproduced within a model implying exciton formation in both the host matrix and the emitter molecules, with subsequent triplet-energy transfer between host and guest molecules. These energy-transfer processes are illustrated in Fig. 4. By comparing analytical results with experiments, we conclude that the majority of dark triplet excitons generated in the host matrix transfer onto the guest molecules, where they recombine by emitting phosphorescence. This conclusion is valid when the host-to-guest triplet-energy transfer is the dominant channel of decay of the host triplet population. Triplet transfer from host to guest molecules may occur via the Dexter mechanism [26]. Depending on the change in free energy during this process, the opposite transfer may not be very efficient [6].

The rate equation describing the time evolution of the average density of dark (host) triplets,  $\mathbb{T}(t)$ , and phosphorescent (guest) triplets,  $\Phi(t)$ , can be written as

$$\begin{aligned} \frac{d\mathbb{T}}{dt} &= G_{\mathbb{T}} + \alpha_R \Phi - \Gamma_{\mathbb{T}} \mathbb{T}, \\ \frac{d\Phi}{dt} &= G_{\Phi} + \alpha_F \mathbb{T} - \Gamma_{\Phi} \Phi, \end{aligned} \quad (3)$$

where  $G_{\mathbb{T}}$  and  $G_{\Phi}$  are the respective triplet-generation rates,  $\Gamma_{\mathbb{T}}$  and  $\Gamma_{\Phi}$  are their overall decay constants, and  $\alpha_F$  and  $\alpha_R$  are the forward and reverse host-to-guest triplet-transfer rate constants. As this energy transfer constitutes a decay channel of triplets, one has  $\Gamma_{\mathbb{T}} > \alpha_F$  and  $\Gamma_{\Phi} > \alpha_R$  (see Fig. 4). Rate Eq. (3) ignores the coordinate dependence of the densities and is meant to hold locally. The

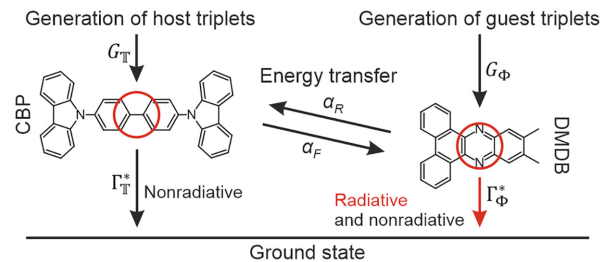


FIG. 4. Triplet dynamics in the host-guest system described by Eq. (3). Rates of forward and reverse transfer,  $\alpha_F$  and  $\alpha_R$ , respectively, and rates of decay from the guest and host triplet states,  $\Gamma_{\Phi}^*$  and  $\Gamma_{\mathbb{T}}^*$ , respectively, are related to the guest and host triplet-decay constants entering into Eq. (3) as  $\Gamma_{\Phi} = \Gamma_{\Phi}^* + \alpha_R$  and  $\Gamma_{\mathbb{T}} = \Gamma_{\mathbb{T}}^* + \alpha_F$ , respectively.



rate of phosphorescence is proportional to the guest triplet-exciton density, so  $\Phi(t)$  is the observable quantity.

### B. Transient electrophosphorescence

Before turning to the analysis of the magnetic resonance experiment illustrated in Fig. 2, we apply the model, Eq. (3), to the transient phosphorescence decay after the device is switched off; this is reported in Ref. [10] for an equivalent device structure. In general, power-law dynamics may occur in the phosphorescence decay at short times when the phosphorescence rate is limited by triplet diffusion to the emitting site [27,28]. However, the phosphorescence transient measured in Ref. [10] is essentially exponential, indicating the nondispersive character of underlying processes. This measurement corresponds to Eq. (3), with generation rates disappearing after  $t = 0$ , which is the time the device is switched off;  $G_{\mathbb{T}}|_{t \geq 0} = 0$ ,  $G_{\Phi}|_{t \geq 0} = 0$ . The resulting solution for the triplet population has the following biexponential form:

$$\Phi(t) = A_1 e^{-k_1 t} + A_2 e^{-k_2 t}, \quad (4)$$

with decay rates

$$k_{1,2} = \frac{\Gamma_{\Phi} + \Gamma_{\mathbb{T}}}{2} \pm \sqrt{\frac{(\Gamma_{\Phi} - \Gamma_{\mathbb{T}})^2}{4} + \alpha_F \alpha_R}. \quad (5)$$

The amplitudes in Eq. (4) are expressed in terms of generation rates before the device is switched off. The measured transient shows a steep drop followed by a monoexponential decay. This behavior is captured by Eq. (4), where  $\Gamma_{\Phi} \gg \Gamma_{\mathbb{T}}$ , entailing  $k_1 \approx \Gamma_{\Phi} \gg k_2$ . With such an arrangement of rates, the last term in Eq. (4) is responsible for the measured monoexponential decay with rate  $k_2$ , which is estimated at  $10.3 \text{ s}^{-1}$ , whereas the first exponent in Eq. (4) contributes to the initial much faster decay of the transient showing up as an unresolved drop in triplet population, and therefore, in phosphorescence intensity.

More useful relationships are found by noting that the natural triplet lifetime in the CBP host is longer than 1 s [6]. This long lifetime indicates that triplet transfer from the CBP matrix to the DMDB emitter is the rate-limiting step in CBP triplet decay, so that the forward transfer rate,  $\alpha_F$ , is very close to (although still smaller than)  $\Gamma_{\mathbb{T}}$ ;  $\alpha_F \approx \Gamma_{\mathbb{T}}$ . Furthermore, judging from the peak positions of the photoluminescence spectra [10], the triplet-energy level of the host is higher than that of the emitter, entailing  $\alpha_F > \alpha_R$ . This conclusion is in agreement with the determination of the host's triplet-energy level by Baldo and Forrest [6]. Thus, we find that, in this regime, the actual value of  $\alpha_R$  has a negligible impact on the phosphorescence dynamics,

and we have

$$k_1 \approx \Gamma_{\Phi} \gg k_2 \approx \Gamma_{\mathbb{T}} \approx \alpha_F \approx 10.3 \text{ s}^{-1}. \quad (6)$$

To summarize the discussion of the phosphorescence transient reported in Ref. [10], we note that it does not show any sign of diffusion-limited delayed phosphorescence [6], thus supporting the validity of our model, Eq. (3), and hence, excluding the possibility of substantial spatial inhomogeneity of the triplet densities within the OLED active layer. Regarding the homogeneity of triplet emitters, we also note that the guest material's concentration in our device is more than 100 times greater than that in earlier work on triplet diffusion [27,28], reinforcing the point that diffusion is unlikely to be very significant in the phosphorescent transients.

### C. Phase-sensitive measurements

The sensitivity of  $\Phi(t)$  to the magnetic field stems from  $G_{\Phi}$ ,  $G_{\mathbb{T}}$ , and  $\Gamma_{\Phi}$ , whereas  $\Gamma_{\mathbb{T}}$ ,  $\alpha_F$ , and  $\alpha_R$  are treated as field independent. The field dependence of  $G_{\Phi}$ ,  $G_{\mathbb{T}}$ , and  $\Gamma_{\Phi}$  is the direct consequence of the field dependence of the PP-recombination and the TEP reaction processes, as discussed in Sec. III D. In the field regime under consideration, the rf carrier frequency,  $\omega_0$ , is large, so that the magnetic field dependence of  $G_{\Phi}$ ,  $G_{\mathbb{T}}$ , and  $\Gamma_{\Phi}$  is the average of these quantities over many rf periods. Thus,  $G_{\Phi}$ ,  $G_{\mathbb{T}}$ , and  $\Gamma_{\Phi}$  are time dependent due to modulation of the driving-field amplitude. The frequency of the rf field is also larger than the largest decay rate involved in Eq. (3),  $\omega_0 \gg \Gamma_{\Phi}$ . Furthermore, the processes governing the magnetic field dependence of rates are much faster (typically  $\gtrsim 1 \text{ MHz}$ ) than that of rf modulation, so any deviation in the time dependence of the rates from the rectangular shape of rf modulation is negligible. This time dependence can then be written as

$$\begin{aligned} G_{\Phi}(t) &= G_{\Phi}(B_0) + \delta G_{\Phi}(B_0, B_1)F(t), \\ \Gamma_{\Phi}(t) &= \Gamma_{\Phi}(B_0) + \delta \Gamma_{\Phi}(B_0, B_1)F(t), \\ G_{\mathbb{T}}(t) &= G_{\mathbb{T}}(B_0) + \delta G_{\mathbb{T}}(B_0, B_1)F(t). \end{aligned} \quad (7)$$

This way of writing the relationship naturally separates the rf-induced variations of the rates,  $\delta G_{\Phi}$ ,  $\delta \Gamma_{\Phi}$ , and  $\delta G_{\mathbb{T}}$ , from their bulk values. It is reasonable to expect that the rf-induced variations of the rates constitute small corrections to their absolute values, i.e.,  $\delta G_{\Phi}/G_{\Phi}$ ,  $\delta \Gamma_{\Phi}/\Gamma_{\Phi}$ , and  $\delta G_{\mathbb{T}}/G_{\mathbb{T}} \ll 1$ .

Phase-sensitive detection provides two related quantities: the in-phase and out-of-phase components,  $U = \text{Im}(\mathcal{I})$  and  $V = \text{Re}(\mathcal{I})$ , respectively, where

$$\mathcal{I} = \frac{2\pi}{\tau} \int_0^{\tau} dt \Phi(t) e^{ift}, \quad (8)$$

where  $\tau$  is the integration time and  $f$  is the angular frequency modulation, which is related to the modulation period,  $2T$ , by  $f = \pi/T$ . Depending on the specific experimental conditions, the response of a system to the square-wave-modulated rf excitation can be quite different [29–31]. In the Supplemental Material [23], we show that, under the conditions relevant to our experiment, Eqs. (3), (7), and (8) lead to the following relationships for the (renormalized) signals:

$$\begin{aligned} U &= \frac{\alpha_F(\Gamma_\Phi\Gamma_\mathbb{T} - f^2)}{(f^2 + \Gamma_\Phi^2)(f^2 + \Gamma_\mathbb{T}^2)}\delta G_\mathbb{T} \\ &\quad + \frac{\Gamma_\Phi}{f^2 + \Gamma_\Phi^2}[\delta G_\Phi - \Phi_0\delta\Gamma_\Phi], \\ V &= -\frac{\alpha_F f(\Gamma_\Phi + \Gamma_\mathbb{T})}{(f^2 + \Gamma_\Phi^2)(f^2 + \Gamma_\mathbb{T}^2)}\delta G_\mathbb{T} \\ &\quad - \frac{f}{f^2 + \Gamma_\Phi^2}[\delta G_\Phi - \Phi_0\delta\Gamma_\Phi], \end{aligned} \quad (9)$$

where  $\Phi_0 = (G_\Phi\Gamma_\mathbb{T} + \alpha_F G_\mathbb{T})/(\Gamma_\Phi\Gamma_\mathbb{T} - \alpha_F\alpha_R)$  is the steady-state population of phosphorescent triplets. Equation (9) details the magnetic field dependence of the signals in terms of rf-dependent  $\delta G_\mathbb{T}$ ,  $\delta G_\Phi$ , and  $\delta\Gamma_\Phi$ , which, in turn, are found from the microscopic modeling of the spin dynamics of PP recombination in the host matrix, PP recombination in the guest emitter molecule, and the TEP reaction in the emitter, respectively.

#### D. Magnetic field dependence of rates

Since excitons are recombination products of electron-hole pairs, the triplet-generation rates,  $G_\mathbb{T}$  and  $G_\Phi$ , are governed by the PP mechanism in the host matrix and the guest emitter [cf. Fig. 1(a)]. The decay of triplet excitons, on the other hand, may occur through various more- or less-efficient pathways. Among these pathways, we single out the TEP process between phosphorescent triplets and hole polarons at guest-molecule sites, as the most plausible mechanism controlling the field dependence of  $\Gamma_\Phi$ , and neglect the field dependence of other pathways, including TEP processes involving other polaron species. This choice is motivated by the fact that the host matrix is primarily a hole conductor. The PP and TEP mechanisms relevant to our system are illustrated in Fig. 1. PP recombination is one of the standard mechanisms leading to relatively large magnetic field effects on millitesla (mT) scales [32,33]. It is closely related to the radical-pair mechanism, which accounts for a range of magnetic field effects in biochemical systems [12,13]. The key ingredient of PP recombination is the weakly coulombically coupled bound state of electrically injected electron and hole polarons. The PP state may recombine into an exciton or dissociate back to separate polarons. The recombination process is

spin conserving, so that the resulting exciton is triplet (singlet) if the total spin of the PP is triplet (singlet). The PP is subject to local hyperfine magnetic fields, which differ at individual polaron sites, and therefore, the total spin multiplicity of a PP may change over time. The spin multiplicity of a PP may also be affected by an external magnetic field. Hence, PP recombination, as well as exciton generation, is sensitive to the external magnetic field.

Generation rates of triplets are determined by the triplet contents of PP ensembles in the host (h) material and guest (g) emitters. The two cases should be thought of as PPs recombining either on host- or guest-molecule sites, i.e., the guest PP is not necessarily limited in extension to a single guest molecule within the host. Introducing the spin-density matrices of the corresponding PP ensembles,  $\rho_h$  and  $\rho_g$ , triplet-generation rates can be written as

$$G_\mathbb{T} = r_{\mathbb{T},h} \text{tr}(\rho_h \Pi_{\mathbb{T},h}), \quad G_\Phi = r_{\mathbb{T},g} \text{tr}(\rho_g \Pi_{\mathbb{T},g}), \quad (10)$$

where  $\Pi_{\mathbb{T},\mu}$  are projection operators onto the triplet manifolds and  $r_{\mathbb{T},\mu}$  are the material-specific field-independent coefficients of triplet generation,  $\mu = h, g$ . Thus, the field dependence of  $G_\mathbb{T}$  and  $G_\Phi$  comes from that of  $\rho_h$  and  $\rho_g$ .

The third field-dependent mechanism considered here is the reaction of phosphorescent guest triplets with the hole polarons on guest molecules. The total spin of a TEP complex is either 1/2 (doublet, D) or 3/2 (quartet, Q). The TEP reaction is assumed to be spin conserving, so that doublet states may recombine into a separate molecular singlet state and a polaron, whereas recombination from quartet states is forbidden. The recombination process occurs with the rate  $r_D \text{tr}(\varrho \Pi_D)$ , where  $\varrho$  is the spin-density matrix of the ensemble of guest TEPs,  $\Pi_D$  is the projection operator onto the doublet manifold of the ensemble, and  $r_D$  is the recombination rate of doublet states. As this recombination contributes to the total population decay of triplet excitons by phosphorescence, we have

$$\Gamma_\Phi \Phi = r_D \text{tr}(\varrho \Pi_D) + \Gamma'_\Phi \Phi, \quad (11)$$

where  $\Gamma'_\Phi$  is the magnetic-field-independent part of  $\Gamma_\Phi$ .

The time evolution of the density matrices  $\rho_\mu$  ( $\mu = h, g$ ) and  $\varrho$  is described by the stochastic Liouville equations

$$\frac{d\rho_\mu}{dt} = \Lambda_\mu \mathbb{1}_{4\times 4} + i[\rho_\mu, H_{\text{PP},\mu}] + \mathcal{R}_{\text{dr}}\{\rho_\mu\} + \mathcal{R}_{\text{sl}}\{\rho_\mu\}, \quad (12)$$

$$\frac{d\varrho}{dt} = \Lambda_{\text{TEP}} \mathbb{1}_{6\times 6} + i[\varrho, H_{\text{TEP}}] + \mathcal{R}_{\text{dr}}\{\varrho\} + \mathcal{R}_{\text{sl}}\{\varrho\}, \quad (13)$$

where the first terms, with  $\mathbb{1}_{4\times 4}$  and  $\mathbb{1}_{6\times 6}$  representing the  $4 \times 4$  and  $6 \times 6$  identity operators, describe PP and TEP-complex generation with the rates  $\Lambda_\mu$  ( $\mu = h, g$ ) and  $\Lambda_{\text{TEP}}$ . The second terms capture the coherent spin dynamics

due to the magnetic interactions governed by the (time-dependent) spin Hamiltonians,  $H_{PP, \mu}$  ( $\mu = h, g$ ) and  $H_{TEP}$ , with  $\mathcal{R}_{dr}$  representing dissociation and recombination and  $\mathcal{R}_{sl}$  representing spin-lattice relaxation. Note that Eq. (12) is a  $4 \times 4$  matrix differential equation and Eq. (13) is a  $6 \times 6$  one.

The Supplemental Material [23] contains an in-depth analysis of Eqs. (10)–(13), yielding the field dependence of  $\delta G_T$ ,  $\delta G_\Phi$ , and  $\delta \Gamma_\Phi$ . We find the respective resonance lines utilizing solutions to the stochastic Liouville equations based on the Floquet theorem, a framework that has proved to be very convenient for numerical simulations [14,23]. We find that in the low-magnetic-field regime, this approach is more reliable, although theoretically somewhat more demanding than the conventional rotating-wave approximation [14]. The following general characterization can be given regarding the numerically established resonance lines. Quite intuitively, the PP-induced resonance lines can be closely approximated by double Gaussians, with the individual Gaussians arising from the constituent polaron species. This approximation is in accordance with the semiclassical picture of electron-nuclear-spin coupling in organic semiconductors [34] observed in many experiments (see, e.g., Refs. [35,36]). The individual Gaussians retain clear fingerprints of the underlying polaron spin states, featuring linewidths close to the strengths of the polaron-spin hyperfine coupling and resonance-peak centers roughly following the slightly different  $g$  factors of the two polaron spins (see the Supplemental Material [23] for more details). One subtlety in the intuitive picture of this double-Gaussian approximation is that the relative weight of the two Gaussian lines deviates from unity. This deviation cannot be rationalized from considerations regarding the individual polaron spins but can be attributed to spin-spin coupling within the PPs. Our numerical simulations confirm that the deviation is due to the polaron-spin dipolar and exchange couplings, showing that the double-Gaussian approximation is asymptotically exact at the limit of vanishing spin-spin coupling. In the regime under consideration, the TEP-induced line is closely approximated by a single Gaussian, resulting from the polaron-spin resonance, whereas the resonance features of the triplet exciton are completely washed out. This obscuring arises because of the powder averaging of triplet states, which are characterized by the so-called zero-field interaction [see Eq. (S24) within the Supplemental Material [23]]. More specifically, the zero-field splitting (ZFS) parameters  $D$  and  $E$  of guest (DMDB) triplets are expected to be a few tens of mT in strength. In our calculations, we utilized  $D_{ZFS} = 75$  mT and  $E_{ZFS} = 0.13D_{ZFS}$  (these values were established experimentally, by electron-spin-resonance spectroscopy, for a phenazine-based phosphorescent emitter structurally similar to DMDB [37]). With the unusually large ratios of zero-field parameters and the rf ( $D_{ZFS}/\hbar\omega_0 \approx 7.5$  and  $E_{ZFS}/\hbar\omega_0 \approx 1$ ), the half-field

triplet resonance is absent and the full-field triplet resonance is smeared out [38], and therefore, not discernible in comparison to the sharp spin-1/2 polaron resonance.

## IV. FITTING OF SIMULATIONS TO ODMR SPECTRA

### A. Phosphorescence channel

The best agreement between the model and experimentally measured phosphorescence ODMR lines is shown in Fig. 5. The specific parameters used in the simulations of the PP and TEP components are listed in Table S1 within the Supplemental Material [23]. We work in the regime where the effective spin-lattice relaxation is slow (with relaxation times of a few microseconds), so that the spin dynamics is predominantly governed by coherent recombination-dissociation processes. Furthermore, the best fit is achieved by invoking slightly different  $g$  factors for electron and hole polarons in the PP processes (see Table S1 within the Supplemental Material [23]). The  $g$  factor of the hole polarons involved in the PP process is also different from that of the hole polarons in the TEP mechanism (recall that the TEP process considered here involves only hole polarons). These slight differences in  $g$  factor are attributed to the different electronic structures of the three polaronic states, entailing different corrections from the weak but finite spin-orbital coupling, as supported

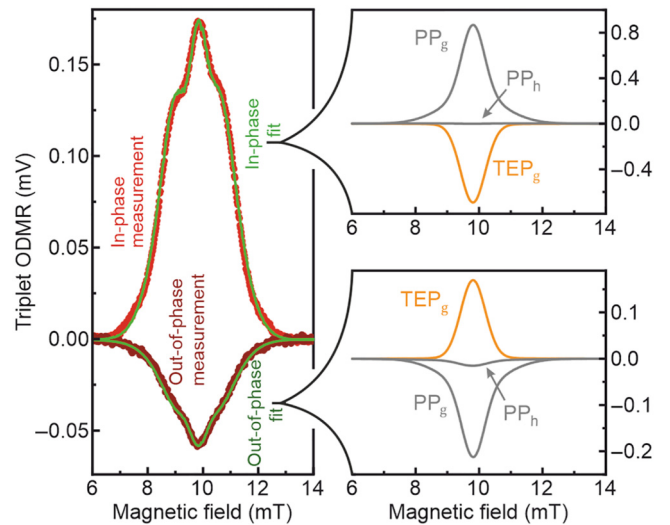


FIG. 5. Left, experimentally measured in-phase and out-of-phase phosphorescence ODMR lines are plotted together with best-fit simulations (green). Right, host (h) and guest (g) PP-induced components,  $PP_h \sim \delta G_T$  and  $PP_g \sim \delta G_\Phi$ , and the TEP component,  $TEP_g \sim \delta \Gamma_\Phi$ , of the simulated lines are shown. Individual lines are different between the upper and lower right panels only because of the different multiplicative factors given in Eq. (9). In spite of the apparently small weight, the  $PP_h$  component is responsible for the deviation of in-phase and out-of-phase lineshapes.

by prior density-functional-theory calculations and high-field magnetic resonance spectroscopy [39]. It is important to mention that the specific shape of the resonance lines recorded appears to be highly restrictive with respect to the internal parameters defining the components of the PP and TEP mechanisms, rendering the fitting procedure quite unambiguous. The relative weights of the PP and TEP components in the signals detected, analytically described by Eq. (9), are numerically found in the course of fitting. The fact that the TEP component enters only into the  $\delta\Gamma_\Phi$  factors of Eq. (9) allows us to extract the as-yet-unknown decay constant,  $\Gamma_\Phi$ , without resorting to  $\Gamma_\mathbb{T}$ ,

$$\Gamma_\Phi = 2.4 \times 10^3 \text{ s}^{-1}. \quad (14)$$

This rate is essentially the inverse phosphorescence lifetime of the guest triplet exciton. The result in Eq. (14) is in full agreement with Eq. (6), verifying  $\Gamma_\Phi \gg \Gamma_\mathbb{T}$ .

### B. Fluorescence channel

The signal detected in the out-of-phase channel of fluorescence is 2 orders of magnitude smaller than the in-phase fluorescence signal, with a poor signal-to-noise ratio. This is expected, as the fluorescence is much faster than the rf modulation. Therefore, our analysis of the fluorescence line, summarized in Fig. 6, focuses only on the in-phase component. Singlet-exciton generation from a PP process is complementary to triplet generation from the same PP process, so it is natural to expect that the PP constituents of the fluorescence resonance line are the same as those of the phosphorescence,  $\delta G_\mathbb{T}$  and  $\delta G_\Phi$ . However, we are unable to fit the measured fluorescence line with just  $\delta G_\mathbb{T}$  and  $\delta G_\Phi$ . Instead, a very close fit is obtained by combining the  $\delta G_\Phi$  and  $\delta\Gamma_\Phi$  lines, as shown in Fig. 6. Moreover, as seen in Fig. 6, the contribution of the TEP-induced  $\delta\Gamma_\Phi$  to the fluorescence ODMR line is quite significant.

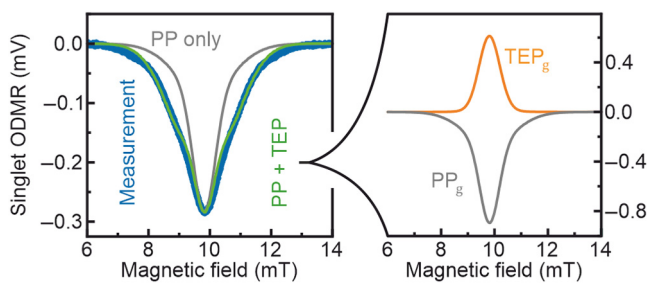


FIG. 6. Fit of the in-phase fluorescence resonance line (left panel). Agreement between measurement (blue) and theory (green) is very good when the guest PP- and TEP-induced lines are both involved, whereas the guest PP line on its own (gray) is nowhere close to the measurement. Guest  $\text{PP}_g \sim \delta G_\Phi$  and  $\text{TEP}_g \sim \delta\Gamma_\Phi$  resonances, comprising the fit, are shown in the right-hand panel. These lines differ from those in the right-hand panels of Fig. 5 only by normalization.

The procedure of finding the best-fitting simulation demonstrates that, in addition to singlet generation from guest PP recombination, fluorescent singlets are produced in the course of the TEP reaction on the guest molecule. This process of singlet generation is illustrated schematically in Fig. 1. Two different TEP reactions are shown, triplet upconversion and triplet quenching, which share the same spin dynamics but yield different reaction products. In the upconversion process induced by the TEP mechanism, the triplet is converted into a higher-energy singlet at the expense of polaron energy. In contrast, the triplet is destroyed, and its energy is transferred to the polaron in the quenching process induced by the TEP mechanism. As the spin dynamics of the two reactions are basically identical, with both reactions resulting in the reduction of the triplet population, the  $\delta\Gamma_\Phi$  line initially found in the phosphorescence ODMR spectrum can be attributed to either of the two processes, and it is the fluorescence channel of the ODMR that probes the difference between the two mechanisms. The fit in Fig. 6 implies the presence of a component due to the TEP interaction in the fluorescence channel, thus supporting the scenario of upconversion.

### V. DISCUSSION

OLEDs comprising an emitting layer of CBP:DMDB enable the detection of both fluorescence and phosphorescence with comparable brightness and sufficient spectral separation. In our earlier study [10], different device structures were tested and it was noted that additional hole- and electron-blocking layers might increase the external quantum efficiency, allowing for a higher signal-to-noise ratio. Compared to the best device reported in Ref. [10], here, we used a stack layout with an additional poly(3,4-ethylenedioxythiophene)/polystyrene sulfonate (PEDOT:PSS) layer, improving charge-carrier injection. Furthermore, layer thicknesses were optimized to achieve the best ODMR signal quality. OLEDs optimized in this way show improved data quality, allowing us to observe phosphorescence ODMR spectra at a high resolution unattainable with the previously reported device structures [3,10].

Our best-fitting numerical simulations of the phosphorescence ODMR lines involve three different components: two PP-induced lines from the host and guest materials and one TEP-induced line resulting from triplet excitons on the guest molecules and hole polarons in the host. The different lineshapes of in-phase and quadrature signals observed in the phosphorescence channel are found to be caused by triplet excitons formed in the host matrix and subsequently transferred to guest chromophores. At the same time, triplet excitons are also formed directly on guest chromophores, as follows from our theoretical analysis. This model contrasts with that of Ref. [5], where the very high internal quantum efficiency of an Ir-based phosphorescent



OLED was attributed to direct exciton formation at the guest phosphor embedded in an electron-transporting host layer.

Ascribing the polaron constituent of the TEP mechanism to the host's hole polaron is motivated by the high concentration of host molecules and by the fact that the host is a good hole conductor. One way to distinguish between guest and host polarons conclusively would be to selectively deuterate both materials and, crucially, perform frequency-dependent measurements to discriminate any inherent difference in the underlying lineshape due to, e.g., spin-orbit coupling. This is, however, far beyond the scope of the present work.

We differentiate TEP-induced triplet quenching from TEP-induced triplet upconversion. These triplet deactivation processes have indistinguishable spin dynamics but are microscopically very different. In particular, in an oversimplified picture, the precursor triplet-exciton-polaron state in the quenching process is thought to involve a trapped polaron and a triplet, which may also be localized. The precursor state in the upconversion process, on the other hand, must involve a free polaron of higher energy, which is transferred to the triplet to convert it into a higher-energy singlet. Thus, the precursor state of quenching is more likely to have a lifetime long enough (at least a few hundred nanoseconds) to render the process sensitive to millitesla magnetic fields. The precursor state of the upconversion process, which is implied to be the scattering of a free polaron by a trapped triplet, in contrast, is expected to be very short lived. Despite the issue of requiring a precursor state, the TEP-induced upconversion mechanism has been subject to extensive consideration in the context of organic semiconductors [2,17–19,21]. Our theoretical analysis of fluorescence ODMR lines reveals a sizable TEP component in singlet generation, which we assign to upconversion. The absence of delayed fluorescence from our OLEDs, which would be a signature of triplet-triplet annihilation, also provides support in favor of the upconversion mechanism. This experimental observation narrows down the possible sources of singlet-exciton generation substantially, excluding processes like (reverse) intersystem crossing from triplet to singlet (i.e., by thermally activated delayed fluorescence [40,41]) and triplet-triplet annihilation into a singlet [20,42]. As for TEP-induced upconversion, this mechanism cannot contribute to any kind of delayed response, as it relies on the availability of high-energy polarons, which are necessarily short lived.

## VI. CONCLUSIONS

ODMR is an exceptionally powerful technique to track spin-dependent processes in OLEDs. In combination with a dual singlet-triplet-emitting material, the conversion between singlet and triplet states can be tracked directly

by monitoring fluorescence and phosphorescence yields. Although many of the magnetic field effects of OLEDs can be rationalized by the mixing between singlet- and triplet-carrier pair-precursor states in local hyperfine fields [8,11], i.e., the PP mechanism, in these DMDB OLEDs, the PP mechanism on its own is clearly not sufficient to describe spin interconversion. The TEP mechanism occurs in addition to the PP mechanism, leading to both the suppression of phosphorescence on resonance and the concomitant increase in fluorescence. Clearly, this triplet upconversion to singlets must depend on the energy of the polaron, which, in turn, must be derived from the electric field applied to the OLED. We anticipate that the upconversion process will exhibit a quantitative dependence on both the OLED bias and temperature, since the number of trapped charges available for the quenching TEP reaction should increase with decreasing temperature. Such studies will be important in the future, since there is, as yet, no complete quantum chemical picture of the transient exciton-polaron state formed during the scattering process [2,17–19,21]. Finally, it is intriguing to note the conceptual parallel of the TEP process, giving rise to light emission here, to the electrofluorescent trions observed in single-molecule scanning-tunneling-microscopy experiments [43]. While the latter are clearly strongly bound and confined to one molecule, the transient exciton-polaron state can perhaps be thought of as a weakly bound trion, albeit of triplet excitons. Since charging can alter the transition energies of the molecule [44], it may be possible to uncover features in the actual electrophosphorescence spectrum that are associated with this transiently bound trionlike feature.

## ACKNOWLEDGMENTS

This work is funded by the Deutsche Forschungsgemeinschaft (DFG, German Research Foundation) (project ID 314695032-SFB 1277, subproject B03). The authors thank Hans Malissa for helpful discussions.

- 
- [1] J. Shinar, Optically detected magnetic resonance studies of luminescence-quenching processes in pi-conjugated materials and organic light-emitting devices, *Laser Photonics Rev.* **6**, 767 (2012).
  - [2] V. Ern and R. E. Merrifield, Magnetic field effect on triplet exciton quenching in organic crystals, *Phys. Rev. Lett.* **21**, 609 (1968).
  - [3] T. Grünbaum, S. Milster, H. Kraus, W. Ratzke, S. Kurrmann, V. Zeller, S. Bange, C. Boehme, and J. M. Lupton, OLEDs as models for bird magnetoreception: Detecting electron spin resonance in geomagnetic fields, *Faraday Discuss.* **221**, 92 (2020).
  - [4] T. H. Tennaheva, S. Hosseinzadeh, S. I. Atwood, H. Popli, H. Malissa, J. M. Lupton, and C. Boehme, Spin relaxation dynamics of radical-pair processes at low magnetic fields, arXiv:2207.07086.

- [5] C. Adachi, M. A. Baldo, M. E. Thompson, and S. R. Forrest, Nearly 100% internal phosphorescence efficiency in an organic light-emitting device, *J. Appl. Phys.* **90**, 5048 (2001).
- [6] M. A. Baldo and S. R. Forrest, Transient analysis of organic electrophosphorescence: I. Transient analysis of triplet energy transfer, *Phys. Rev. B* **62**, 10958 (2000).
- [7] H. Yersin, *Highly Efficient OLEDs with Phosphorescent Materials* (Wiley, Weinheim, 2007).
- [8] H. Kraus, S. Bange, F. Frunder, U. Scherf, C. Boehme, and J. M. Lupton, Visualizing the radical-pair mechanism of molecular magnetic field effects by magnetic resonance induced electrofluorescence to electrophosphorescence interconversion, *Phys. Rev. B* **95**, 241201 (2017).
- [9] D. Chaudhuri, E. Sigmund, A. Meyer, L. Röck, P. Klemm, S. Lautenschlager, A. Schmid, S. R. Yost, T. Van Voorhis, S. Bange *et al.*, Metal-free OLED triplet emitters by side-stepping Kasha's rule, *Angew. Chem., Int. Ed.* **52**, 13449 (2013).
- [10] W. Ratzke, S. Bange, and J. M. Lupton, Direct detection of singlet-triplet interconversion in OLED magnetoelectroluminescence with a metal-free fluorescence-phosphorescence dual emitter, *Phys. Rev. Appl.* **9**, 054038 (2018).
- [11] A. J. Schellekens, W. Wagemans, S. P. Kersten, P. A. Bobbert, and B. Koopmans, Microscopic modeling of magnetic-field effects on charge transport in organic semiconductors, *Phys. Rev. B* **84**, 075204 (2011).
- [12] T. Ritz, S. Adem, and K. Schulten, A model for photoreceptor-based magnetoreception in birds, *Biophys. J.* **78**, 707 (2000).
- [13] U. E. Steiner and T. Ulrich, Magnetic-field effects in chemical-kinetics and related phenomena, *Chem. Rev.* **89**, 51 (1989).
- [14] S. Jamali, V. V. Mkhitaryan, H. Malissa, A. Nahlawi, H. Popli, T. Grünbaum, S. Bange, S. Milster, D. Stoltzfus, A. E. Leung *et al.*, Floquet spin states in OLEDs, *Nat. Commun.* **12**, 465 (2021).
- [15] W. J. Baker, T. L. Keevers, J. M. Lupton, D. R. McCamey, and C. Boehme, Slow hopping and spin dephasing of coulombically bound polaron pairs in an organic semiconductor at room temperature, *Phys. Rev. Lett.* **108**, 267601 (2012).
- [16] K. Kanemoto, S. Hatanaka, K. Kimura, Y. Ueda, and H. Matsuoka, Field-induced dissociation of electron-hole pairs in organic light emitting diodes monitored directly from bias-dependent magnetic resonance techniques, *Phys. Rev. Mater.* **1**, 022601 (2017).
- [17] P. Desai, P. Shakya, T. Kreouzis, W. P. Gillin, N. A. Morley, and M. R. J. Gibbs, Magnetoresistance and efficiency measurements of Alq(3)-based OLEDs, *Phys. Rev. B* **75**, 094423 (2007).
- [18] T. L. Keevers, W. J. Baker, and D. R. McCamey, Theory of exciton-polaron complexes in pulsed electrically detected magnetic resonance, *Phys. Rev. B* **91**, 205206 (2015).
- [19] A. Obolda, Q. M. Peng, C. Y. He, T. Zhang, J. J. Ren, H. W. Ma, Z. G. Shuai, and F. Li, Triplet-polaron-interaction-induced upconversion from triplet to singlet: A possible way to obtain highly efficient OLEDs, *Adv. Mater.* **28**, 4740 (2016).
- [20] R. E. Merrifield, Magnetic effects on triplet exciton interactions, *Pure Appl. Chem.* **27**, 481 (1971).
- [21] S. Chen and H. Xu, Electroluminescent materials toward near ultraviolet region, *Chem. Soc. Rev.* **50**, 8639 (2021).
- [22] W. J. Baker, D. R. McCamey, K. J. van Schooten, J. M. Lupton, and C. Boehme, Differentiation between polaron-pair and triplet-exciton polaron spin-dependent mechanisms in organic light-emitting diodes by coherent spin beating, *Phys. Rev. B* **84**, 165205 (2011).
- [23] See the Supplemental Material at <http://link.aps.org/supplemental/10.1103/PhysRevApplied.20.044076> for details on sample fabrication, data acquisition, theoretical modeling, and a full description of the numerical procedure. It also includes Refs. [14,15,34,37,38,45–48].
- [24] T. Scharff, W. Ratzke, J. Zipfel, P. Klemm, S. Bange, and J. M. Lupton, Complete polarization of electronic spins in OLEDs, *Nat. Commun.* **12**, 2071 (2021).
- [25] M. Kavand, D. Baird, K. van Schooten, H. Malissa, J. M. Lupton, and C. Boehme, Discrimination between spin-dependent charge transport and spin-dependent recombination in pi-conjugated polymers by correlated current and electroluminescence-detected magnetic resonance, *Phys. Rev. B* **94**, 075209 (2016).
- [26] D. L. Dexter, A theory of sensitized luminescence in solids, *J. Chem. Phys.* **21**, 836 (1953).
- [27] M. Reufer, M. J. Walter, P. G. Lagoudakis, B. Hummel, J. S. Kolb, H. G. Roskos, U. Scherf, and J. M. Lupton, Spin-conserving carrier recombination in conjugated polymers, *Nat. Mater.* **4**, 340 (2005).
- [28] M. Reufer, P. G. Lagoudakis, M. J. Walter, J. M. Lupton, J. Feldmann, and U. Scherf, Evidence for temperature-independent triplet diffusion in a ladder-type conjugated polymer, *Phys. Rev. B* **74**, 241201(R) (2006).
- [29] E. Lifshitz, L. Fradkin, A. Glozman, and L. Langof, Optically detected magnetic resonance studies of colloidal semiconductor nanocrystals, *Annu. Rev. Phys. Chem.* **55**, 509 (2004).
- [30] D. M. G. Leite, A. Batagin-Neto, O. Nunes-Neto, J. A. Gomez, and C. F. O. Graeff, Electrically detected magnetic resonance modeling and fitting: An equivalent circuit approach, *J. Appl. Phys.* **115**, 034510 (2014).
- [31] S.-Y. Lee, S. Paik, D. R. McCamey, and C. Boehme, Modulation frequency dependence of continuous-wave optically/electrically detected magnetic resonance, *Phys. Rev. B* **86**, 11 (2012).
- [32] R. Haberkorn and W. Dietz, Theory of spin-dependent recombination in semiconductors, *Solid State Commun.* **35**, 505 (1980).
- [33] D. Kaplan, I. Solomon, and N. F. Mott, Explanation of large spin-dependent recombination effect in semiconductors, *J. Phys., Lett.* **39**, 51 (1978).
- [34] K. Schulten and P. G. Wolynes, Semiclassical description of electron spin motion in radicals including the effect of electron hopping, *J. Chem. Phys.* **68**, 3292 (1978).
- [35] S. Milster, T. Grünbaum, S. Bange, S. Kurrmann, H. Kraus, D. Stoltzfus, P. L. Burn, A. Leung, T. Darwish, C. Boehme *et al.*, Perdeuterated conjugated polymers for ultralow-frequency magnetic resonance of OLEDs, *Angew. Chem., Int. Ed.* **59**, 9388 (2020).
- [36] H. Malissa, M. Kavand, D. P. Waters, K. J. van Schooten, P. L. Burn, Z. V. Vardeny, B. Saam, J. M. Lupton, and

- C. Boehme, Room-temperature coupling between electrical current and nuclear spins in OLEDs, *Science* **345**, 1487 (2014).
- [37] H. Matsuoka, M. Retegan, L. Schmitt, S. Hoger, F. Neese, and O. Schiemann, Time-resolved electron paramagnetic resonance and theoretical investigations of metal-free room-temperature triplet emitters, *J. Am. Chem. Soc.* **139**, 12968 (2017).
- [38] N. M. Atherton, *Electron Spin Resonance* (Halstead, New York, 1973).
- [39] H. Malissa, R. Miller, D. L. Baird, S. Jamali, G. Joshi, M. Bursch, S. Grimme, J. van Tol, J. M. Lupton, and C. Boehme, Revealing weak spin-orbit coupling effects on charge carriers in a pi-conjugated polymer, *Phys. Rev. B* **97**, 161201 (2018).
- [40] J. M. Lupton and J. Klein, Hot band emission and energy transfer in organic electrophosphorescent devices, *Chem. Phys. Lett.* **363**, 204 (2002).
- [41] J. Stehr, J. M. Lupton, M. Reufer, G. Raschke, T. A. Klar, and J. Feldmann, Sub-microsecond molecular thermometry using thermal spin flips, *Adv. Mater.* **16**, 2170 (2004).
- [42] A. Monguzzi, J. Mezyk, F. Scotognella, R. Tubino, and F. Meinardi, Upconversion-induced fluorescence in multicomponent systems: Steady-state excitation power threshold, *Phys. Rev. B* **78**, 195112 (2008).
- [43] J. Doležal, S. Canola, P. Merino, and M. Švec, Exciton-trion conversion dynamics in a single molecule, *ACS Nano* **15**, 7694 (2021).
- [44] B. Doppagne, M. C. Chong, H. Bulou, A. Boeglin, F. Scheurer, and G. Schull, Electrofluorochromism at the single-molecule level, *Science* **361**, 251 (2018).
- [45] J. H. Shirley, Solution of the Schrödinger equation with a Hamiltonian periodic in time, *Phys. Rev.* **138**, B979 (1965).
- [46] V. V. Mkhitarian, D. Danilovic, C. Hippola, M. E. Raikh, and J. Shinar, Comparative analysis of magnetic resonance in the polaron pair recombination and the triplet exciton-polaron quenching models, *Phys. Rev. B* **97**, 035402 (2018).
- [47] W. Wagemans, A. J. Schellekens, M. Kemper, F. L. Bloom, P. A. Bobbert, and B. Koopmans, Spin-spin interactions in organic magnetoresistance probed by angle-dependent measurements, *Phys. Rev. Lett.* **106**, 196802 (2011).
- [48] D. R. McCamey, H. A. Seipel, S. Y. Paik, M. J. Walter, N. J. Borys, J. M. Lupton, and C. Boehme, Spin Rabi flopping in the photocurrent of a polymer light-emitting diode, *Nat. Mater.* **7**, 723 (2008).